Supporting Information

High-efficiency Purification of CH_4 and H_2 Energy Sources Enabled by a Phosphotungstic Acid-supported Os Single-atom Catalyst

Li-Long Zhang,[1†] Ji Zheng,[3†] Jinxing Gu,[4] Zhuochun Huang,[1] Linguo Lu,[2] Hu Li,[1,*] Zhongfang Chen,[2,*] Song Yang,[1,*]

[1] National Key Laboratory of Green Pesticide, Key Laboratory of Green Pesticide and Agricultural Bioengineering, Ministry of Education, State-Local Joint Laboratory for Comprehensive Utilization of Biomass, Center for R&D of Fine Chemicals of Guizhou University, Guiyang, 550025, China

[2] Department of Chemistry, University of Puerto Rico, Rio Piedras Campus, San Juan, PR, USA

[3] College of Chemistry and Materials Science, Guangdong Provincial Key Laboratory of Functional Supramolecular Coordination Materials and Applications, Jinan University, Guangzhou 510632, China

[4] Department of Chemical & Biological Engineering, Monash University, Clayton Campus, Victoria 3800, Australia

[†] Both authors contributed equally to this work.

* Correspondence:

E-mail: hli13@gzu.edu.cn (HL); zhongfang.chen1@upr.edu (ZC); jhzx.msm@gmail.com (SY)

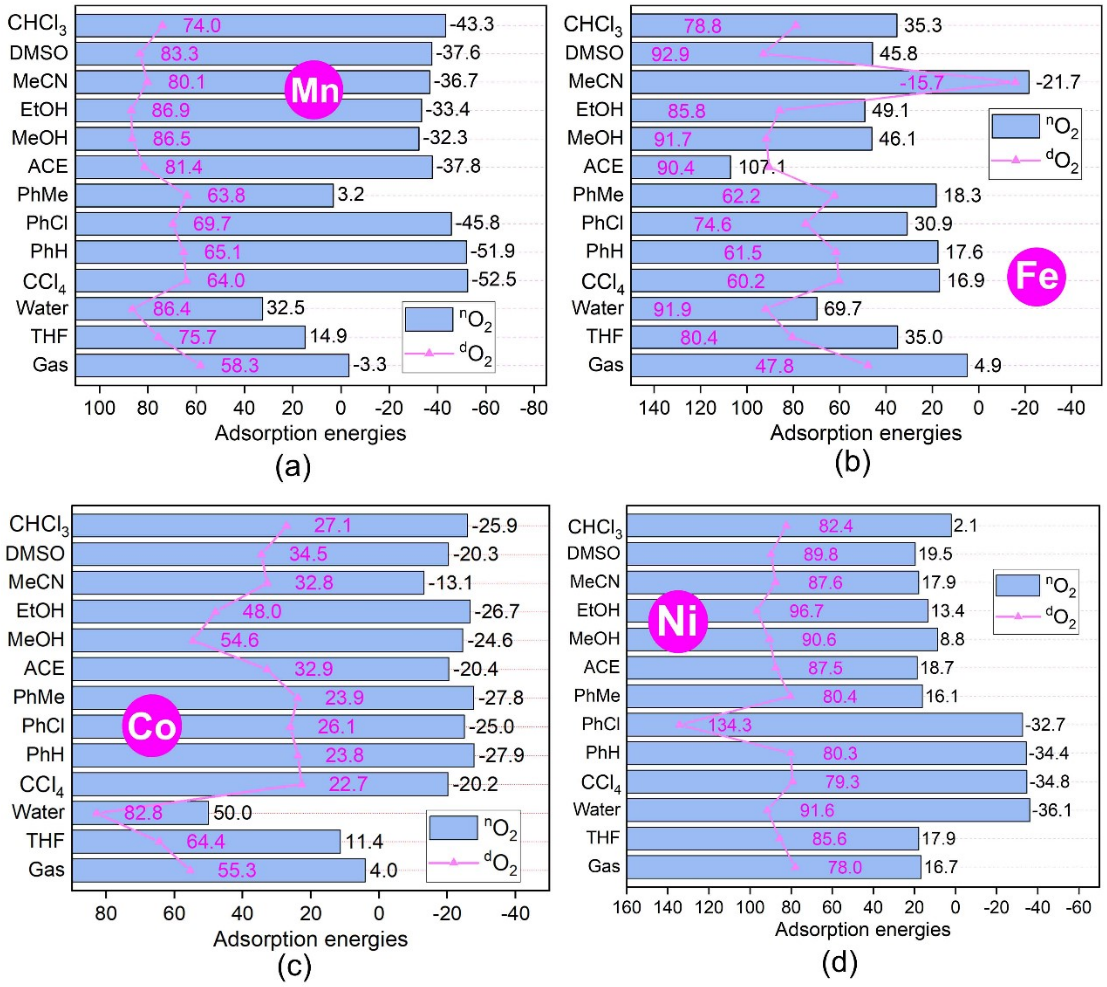

Figure S1. Adsorption free energies of molecular and dissociative adsorption of one O_2 over SACs. Mn_1/PTA (a), Fe_1/PTA (b), Co_1/PTA (c), and Ni_1/PTA (d).

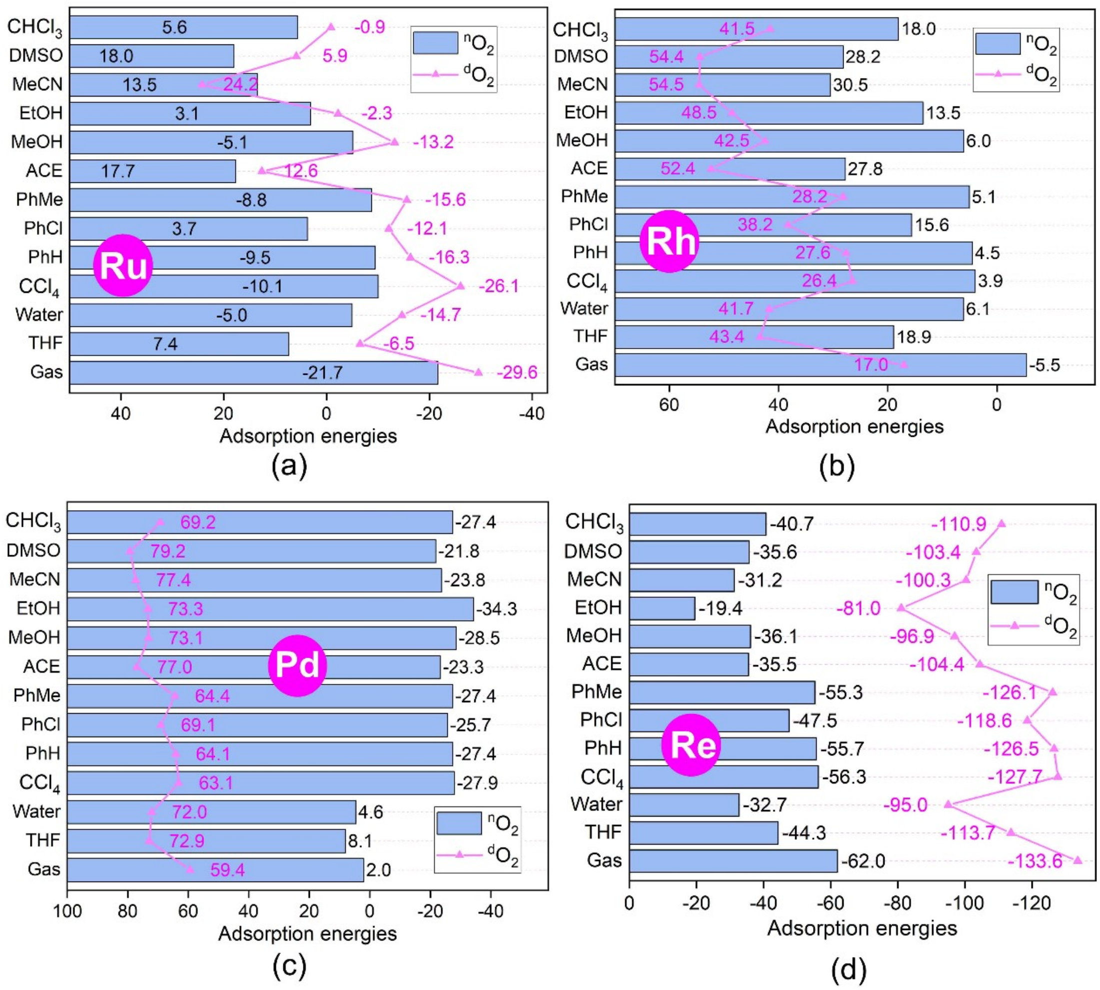

Figure S2. Adsorption free energies of molecular and dissociative adsorption of one O_2 over SACs. Ru_1/PTA (a), Rh_1/PTA (b), Pd_1/PTA (c), and Re_1/PTA (d).

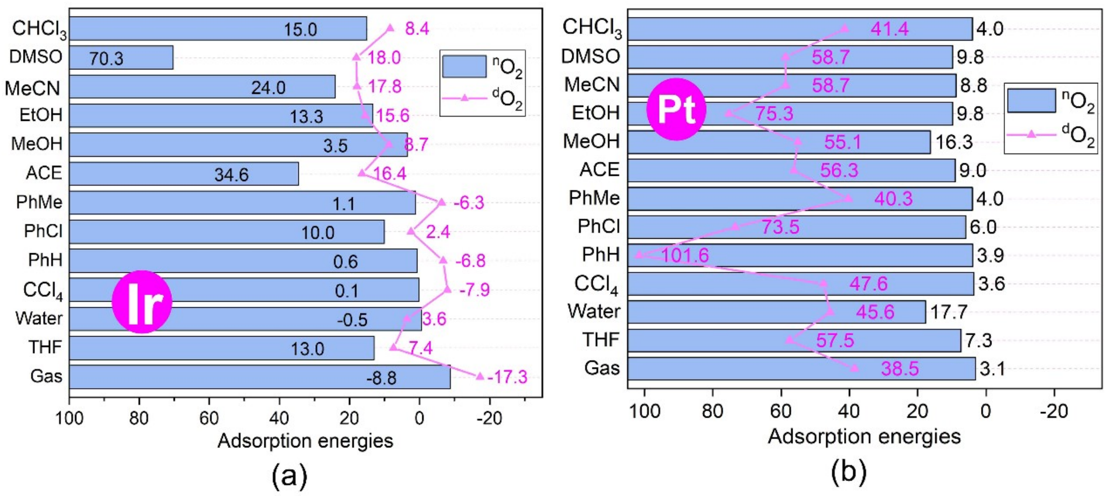

Figure S3. Adsorption free energies of molecular and dissociative adsorption of one O_2 over SACs. Ir_1/PTA (a) and Pt_1/PTA (b).

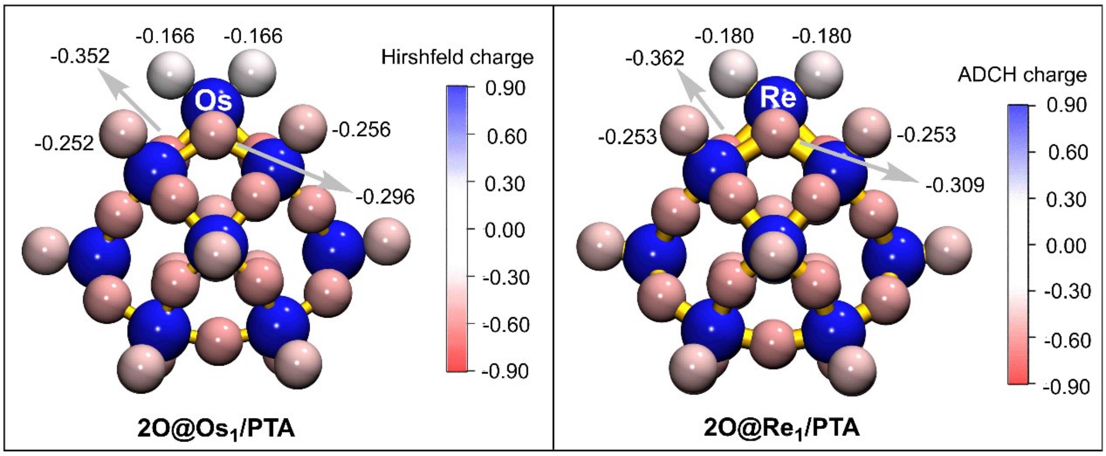

Figure S4. Atomic dipole moment corrected Hirshfeld (ADCH) populations of 2O@Os$_1$/PTA and 2O@Re$_1$/PTA systems (the values of oxygen atoms around the SACs are presented).

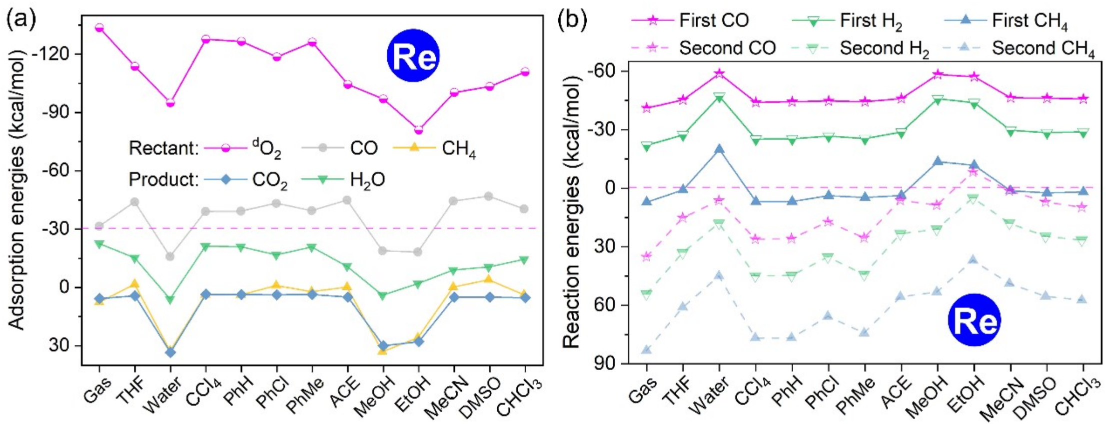

Figure S5. The adsorption free energies of the reactant and product over Re$_1$/PTA (a). The reaction free energies for the first and second CO, H_2 and CH_4 oxidation over Re$_1$/PTA (b).

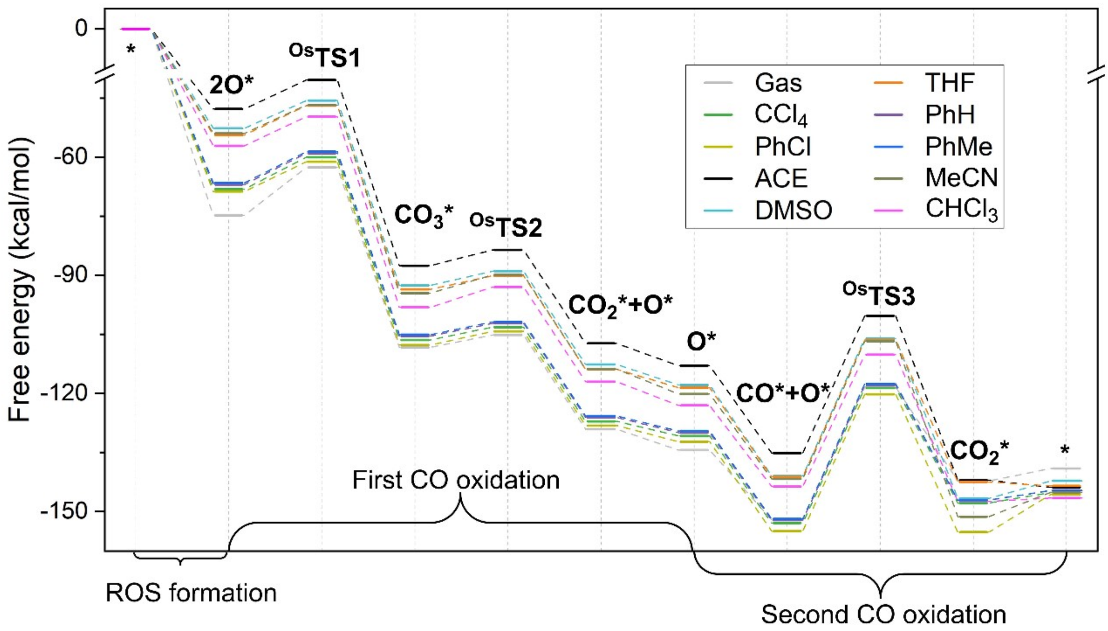

Figure S6. Calculated free energy profiles (in kcal/mol) of CO oxidation over Os_1/PTA SACs in the gas phase and nine solvents.

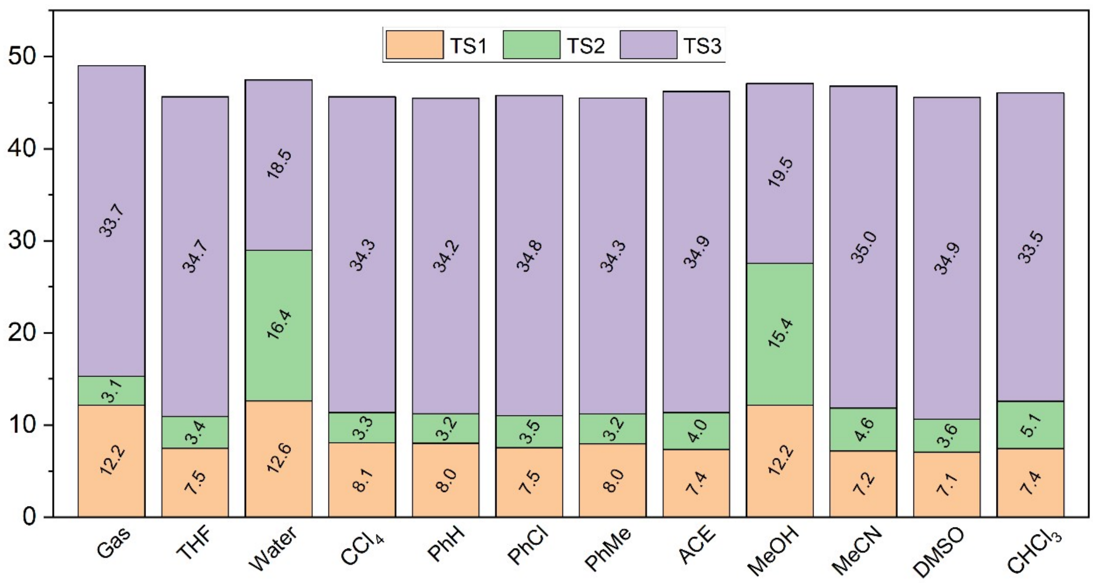

Figure S7. Summed values of **^{Os}TS1**, **^{Os}TS2**, and **^{Os}TS3** over Os_1/PTA SACs in the gas phase and 11 solvents.

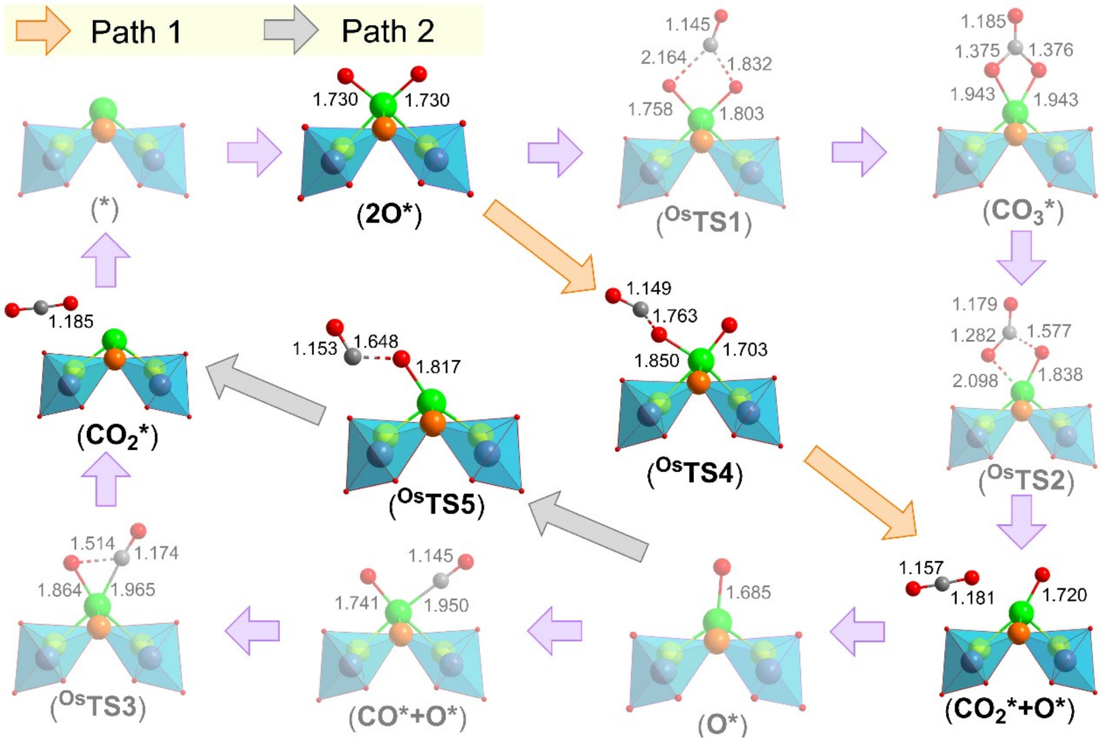

Figure S8. Side pathways of Os_1/PTA SACs-catalyzed CO oxidation.

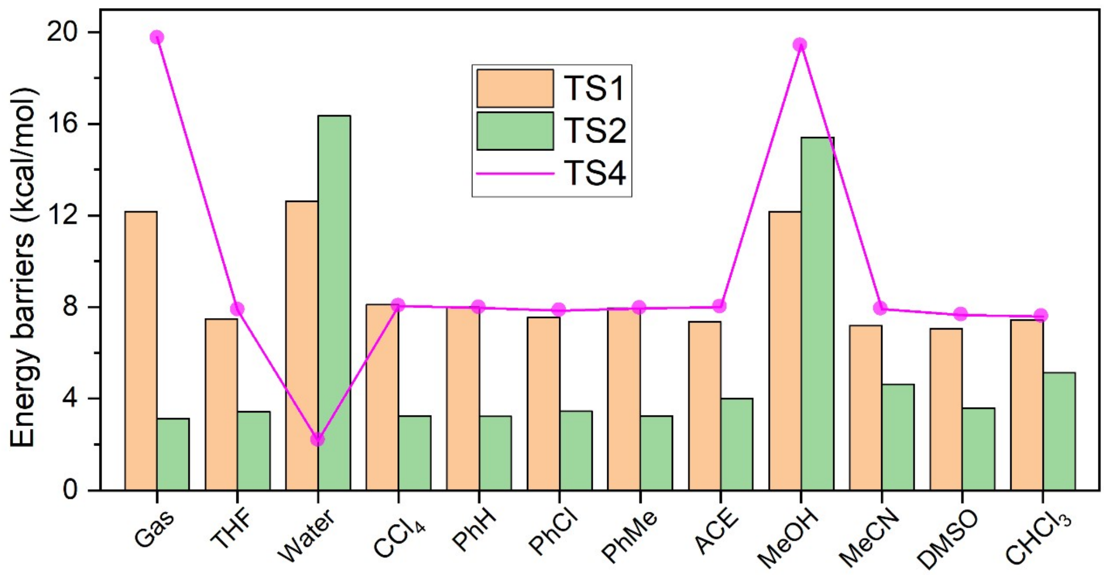

Figure S9. Gibbs free energy barriers of ^{Os}**TS1**, ^{Os}**TS2** and ^{Os}**TS4** in the gas phase and 11 solvents.

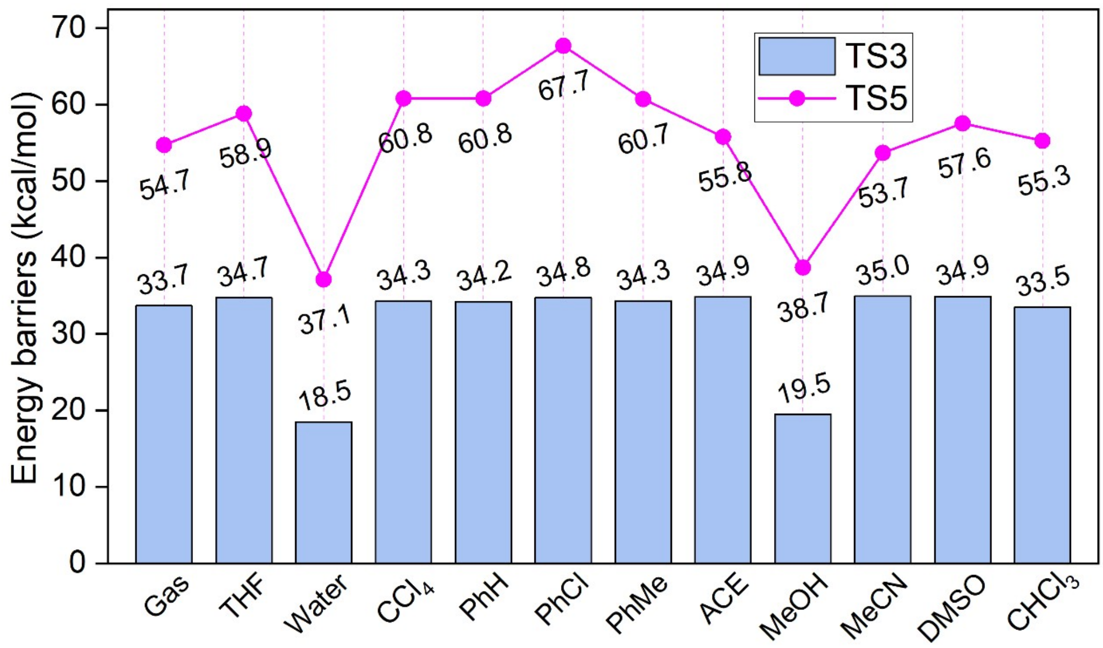

Figure S10. Gibbs free energy barriers of ^{Os}**TS3** and ^{Os}**TS5** in the gas phase and 11 solvents.

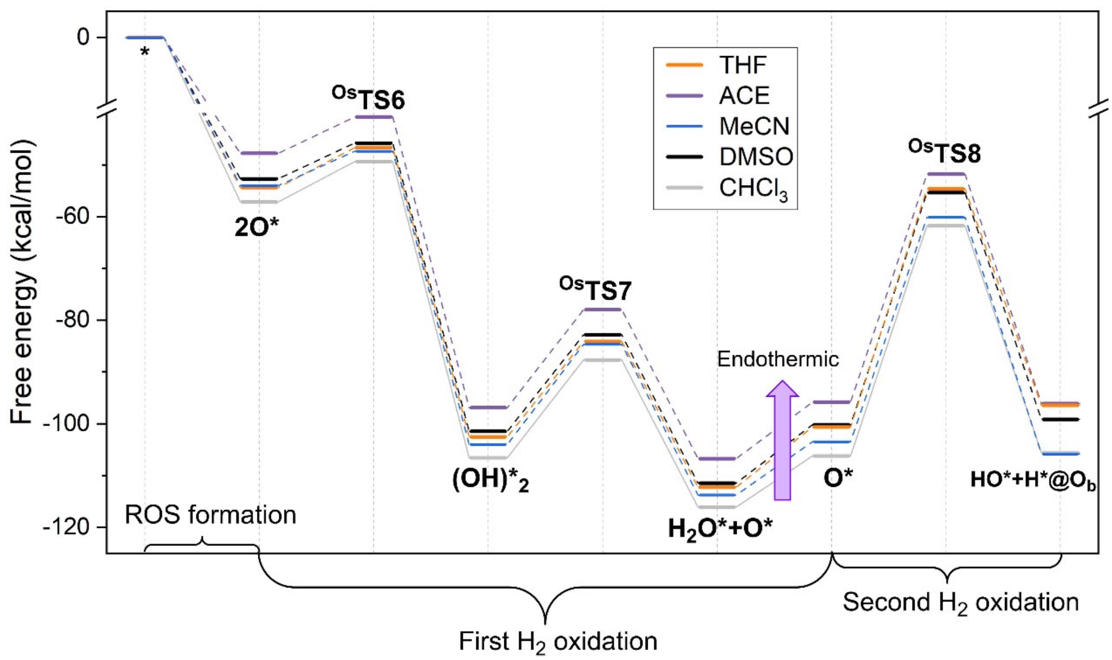

Figure S11. Calculated Gibbs free energy profiles (in kcal/mol) of H_2 oxidation over Os_1/PTA SACs by O_b-bound site in five solvents.

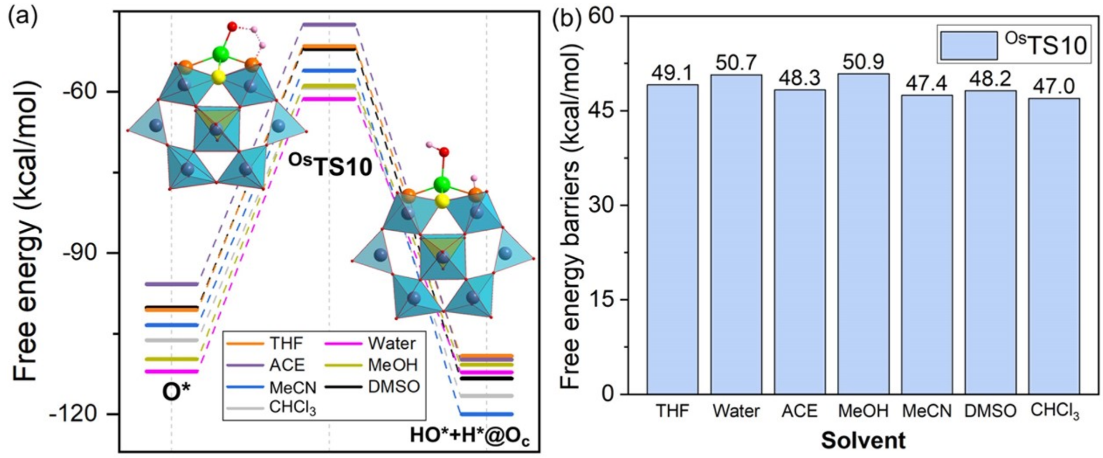

Figure S12. The second H_2 dissociation process by O_c atom in seven solvents (a) and the corresponding free energy barriers (b).

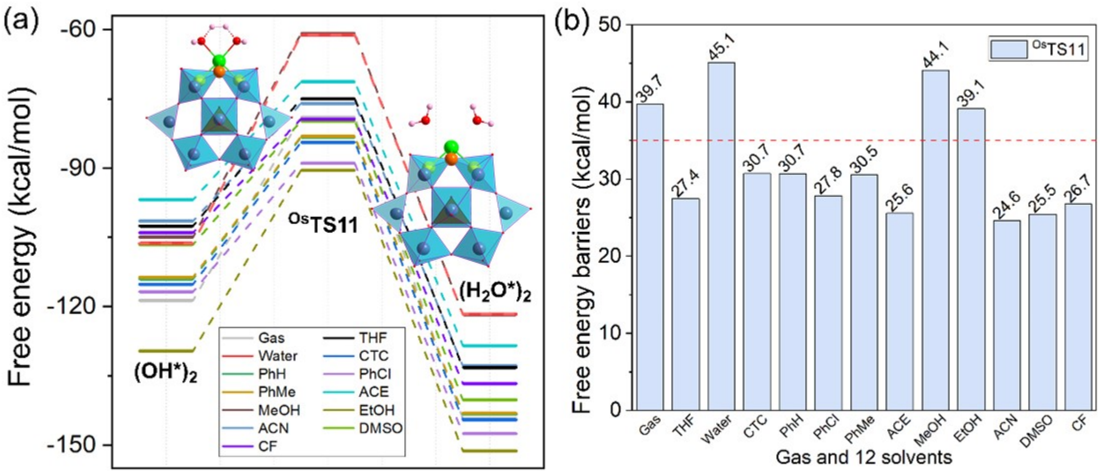

Figure S13. Direct double H_2 oxidation pathway in the gas phase and 12 solvents (a) and the corresponding free energy barriers (b).

The rationale for using the implicit solvation model

Note that our reported computational results are based on implicit solvent models, which are more efficient for large-scale simulations. Considering that explicit solvent models typically provide a finer-grained and more accurate representation of solvation effects, we selected the pivotal intermediate 2O@Os_1/PTA as a representative to examine if the implicit models can give acceptable accuracy for the systems under study. Our calculations revealed that introducing six water molecules onto the catalyst's surface has minimal influence on the lengths of the two Os-O bonds (1.730 Å vs 1.729/1.734 Å, using implicit solvent models as shown in Figure S14). This phenomenon can be attributed to the saturation of the coordination of the Os site. Since the Os sites remain in a saturated state during the crucial step of the entire CO and H_2 oxidation process (Figures 4 and 5), explicit solvent models and implicit solvent models are expected to give us the same trend. Thus, we decided to use the computationally less demanding implicit solvent models throughout this study.

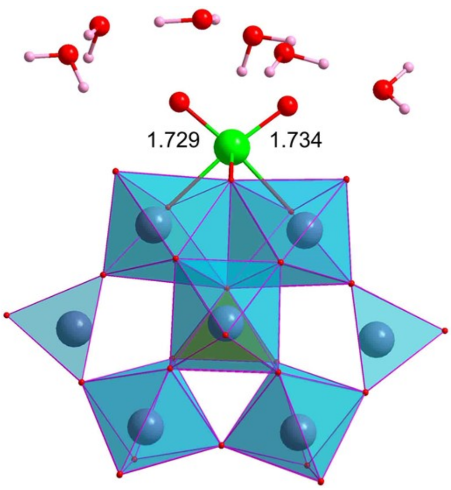

Figure S14. The optimized structure when introducing six water molecules onto the surface of 2O@Os_1/PTA.

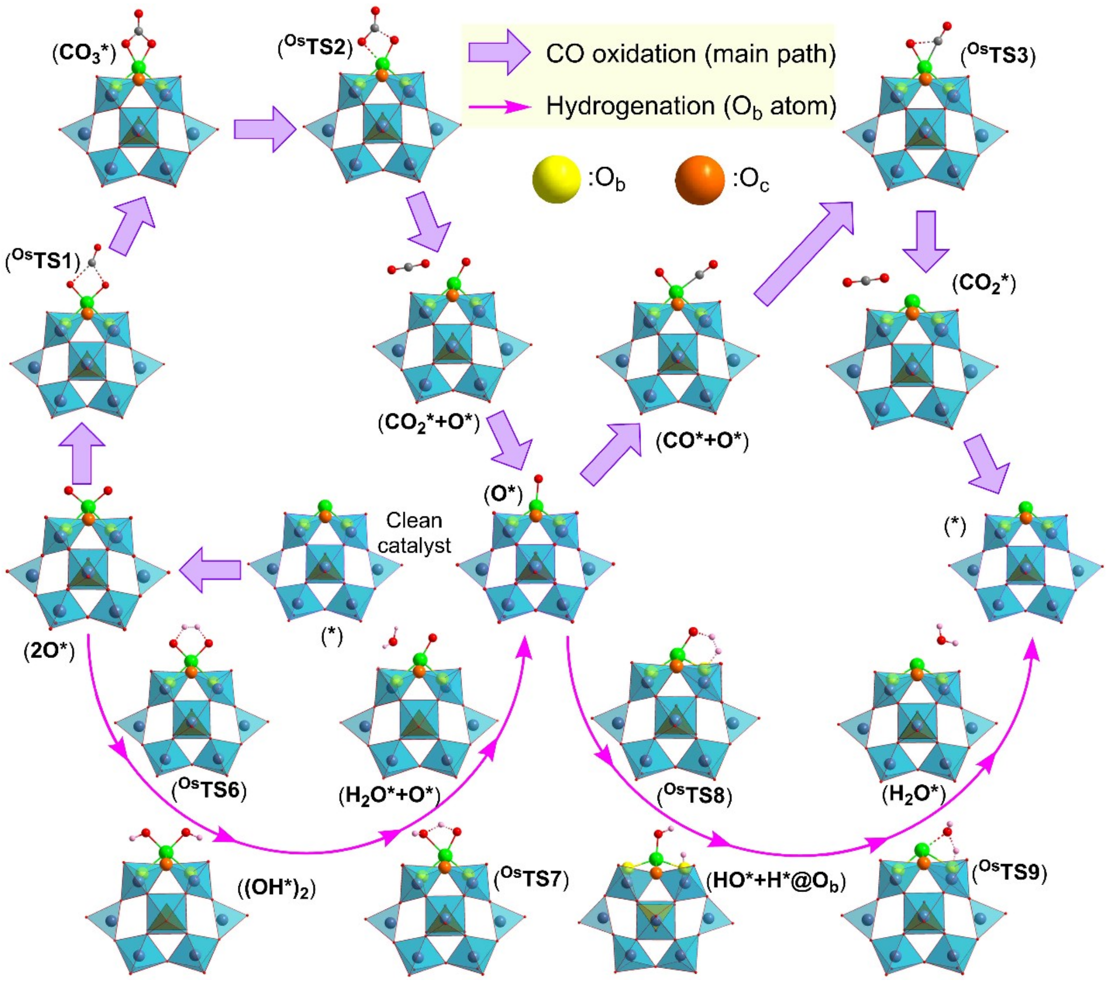

Figure S15. Most favorable catalytic cycles of Os_1/PTA SACs-catalyzed CO and H_2 oxidation in water and MeOH.

Supplementary Table S1. DFT–derived single point energy (in kcal/mol) for the clean M_1/PTA and adsorption complexes with one CH_4, one CO, one CO_2, one H_2O, one normally adsorbed O_2 ($^nO_2$), and one dissociatively adsorbed O_2 ($^dO_2$) with different spin states.

M_1/POM	Spin multiplicity	Total energy (a.u.)	Total energy (kcal/mol)	Relative energy (kcal/mol)
		Clean M_1/POM		
Mn-PTA	1	-4270.51971	-2679793.8	56.5
	3	-4270.56575	-2679822.7	27.6
	5	-4270.60977	-2679850.3	0.0
Fe-PTA	2	-4290.06260	-2692057.2	16.6
	4	-4290.08900	-2692073.8	0.0
	6	-4290.08905	-2692073.8	0.0
Co-PTA	1	-4311.69391	-2705631.0	9.0
	3	-4311.70822	-2705640.0	0.0
	5	-4311.68176	-2705623.4	16.6
Ni-PTA	2	-4335.91927	-2720832.7	0.0
	4	-4335.89153	-2720815.3	17.4
Ru-PTA	2	-4260.44962	-2673474.7	0.0
	4	-4260.44598	-2673472.5	2.3
	6	-4260.42461	-2673459.0	15.7
Rh-PTA	1	-4276.06665	-2683274.6	0.0
	3	-4276.06600	-2683274.2	0.4
	5	-4276.03703	-2683256.0	18.6
Pd-PTA	2	-4293.27934	-2694075.7	0.0
	4	-4293.26462	-2694066.5	9.2
Re-PTA	1	-4245.64559	-2664185.1	0.0
	3	-4245.63651	-2664179.4	5.7
	5	-4245.63991	-2664181.5	3.6
Os-PTA	2	-4257.57246	-2671669.3	0.0
	4	-4257.57145	-2671668.7	0.6
	6	-4257.53900	-2671648.3	21.0
Ir-PTA	1	-4271.21555	-2680230.5	1.5
	3	-4271.21793	-2680232.0	0.0
	5	-4271.16706	-2680200.0	31.9
Pt-PTA	2	-4285.65713	-2689292.7	0.0
	4	-4285.62569	-2689273.0	19.7
		One CH_4		
Mn-PTA	1	-4311.03861	-2705219.8	58.5

	3	-4311.07858	-2705244.9	33.4
	5	-4311.13174	-2705278.3	0.0
Fe-PTA	2	-4330.58106	-2717482.9	23.1
	4	-4330.60689	-2717499.1	6.9
	6	-4330.61792	-2717506.1	0.0
Co-PTA	1	-4352.20648	-2731053.1	8.6
	3	-4352.22016	-2731061.7	0.0
	5	-4352.21048	-2731055.6	6.1
Ni-PTA	2	-4376.43400	-2746256.1	0.0
	4	-4376.41266	-2746242.7	13.4
Re-PTA	1	-4286.16320	-2689610.3	0.0
	3	-4286.15007	-2689602.0	8.2
	5	-4286.15636	-2689606.0	4.3
Ru-PTA	2	-4300.97238	-2698903.2	0.0
	4	-4300.96652	-2698899.5	3.7
	6	-4300.94714	-2698887.3	15.8
Rh-PTA	1	-4316.58986	-2708703.3	0.0
	3	-4316.58332	-2708699.2	4.1
	5	-4316.55919	-2708684.1	19.2
Pd-PTA	2	-4333.79600	-2719500.3	0.0
	4	-4333.78550	-2719493.7	6.6
Os-PTA	2	-4298.09417	-2697097.1	0.0
	4	-4298.08245	-2697089.7	7.4
	6	-4298.05055	-2697069.7	27.4
Ir-PTA	1	-4311.73948	-2705659.6	0.0
	3	-4311.73108	-2705654.4	5.3
	5	-4311.68877	-2705627.8	31.8
Pt-PTA	2	-4326.16903	-2714714.3	0.0
	4	-4326.14604	-2714699.9	14.4
One CH_3OH				
Mn-PTA	1	-4386.27223	-2752429.7	54.1
	3	-4386.31864	-2752458.8	25.0
	5	-4386.35846	-2752483.8	0.0
Fe-PTA	2	-4405.81650	-2764693.9	22.3
	4	-4405.83793	-2764707.4	8.8
	6	-4405.85200	-2764716.2	0.0
Co-PTA	1	-4427.44635	-2778266.9	4.4
	3	-4427.45335	-2778271.3	0.0
	5	-4427.44519	-2778266.1	5.1
Ni-PTA	2	-4451.66267	-2793462.8	0.0
	4	-4451.64735	-2793453.2	9.6
Re-PTA	1	-4361.40554	-2736825.6	0.0
	3	-4361.38315	-2736811.5	14.1
	5	-4361.39191	-2736817.0	8.6

Ru-PTA	2	-4376.20468	-2746112.2	0.0
	4	-4376.19831	-2746108.2	4.0
	6	-4376.17855	-2746095.8	16.4
Rh-PTA	1	-4391.82321	-2755913.0	0.0
	3	-4391.81435	-2755907.4	5.6
	5	-4391.78751	-2755890.6	22.4
Pd-PTA	2	-4409.02888	-2766709.7	0.0
	4	-4409.01246	-2766699.4	10.3
Os-PTA	2	-4373.32876	-2744307.5	0.0
	4	-4373.32019	-2744302.2	5.4
	6	-4373.28666	-2744281.1	26.4
Ir-PTA	1	-4386.97240	-2752869.1	0.0
	3	-4386.96681	-2752865.5	3.5
	5	-4386.92287	-2752838.0	31.1
Pt-PTA	2	-4401.40414	-2761925.1	0.0
	4	-4401.37615	-2761907.6	17.6
		One $^{m}O_2$		
Mn-PTA	1	-4420.88473	-2774149.4	36.8
	3	-4420.94346	-2774186.2	0.0
	5	-4420.93664	-2774182.0	4.3
	7	-4420.92853	-2774176.9	9.4
Fe-PTA	2	-4440.41384	-2786404.1	2.1
	4	-4440.41719	-2786406.2	0.0
	6	-4440.40724	-2786400.0	6.2
	8	-4440.41077	-2786402.2	4.0
Co-PTA	1	-4461.99772	-2799948.2	16.2
	3	-4462.02343	-2799964.3	0.1
	5	-4462.02354	-2799964.4	0.0
	7	-4462.00271	-2799951.3	13.1
Ni-PTA	2	-4486.23638	-2815158.2	0.0
	4	-4486.23490	-2815157.3	0.9
	6	-4486.20389	-2815137.8	20.4
Re-PTA	1	-4396.06972	-2758577.7	0.0
	3	-4396.05660	-2758569.5	8.2
Ru-PTA	2	-4410.79715	-2767819.3	3.1
	4	-4410.80215	-2767822.5	0.0
	6	-4410.76071	-2767796.5	26.0
	8	-4410.74244	-2767785.0	37.5
Rh-PTA	1	-4426.38879	-2777603.2	2.8
	3	-4426.39327	-2777606.0	0.0
	5	-4426.38326	-2777599.8	6.3
	7	-4426.35477	-2777581.9	24.2
Pd-PTA	2	-4443.60144	-2788404.3	0.0
	4	-4443.59585	-2788400.8	3.5

	6	-4443.58295	-2788392.7	11.6
Os-PTA	2	-4407.93810	-2766025.2	9.3
	4	-4407.95296	-2766034.6	0.0
	6	-4407.89337	-2765997.2	37.4
	8	-4407.81315	-2765946.8	50.3
Ir-PTA	1	-4421.55419	-2774569.5	2.3
	3	-4421.55781	-2774571.7	0.0
	5	-4421.53213	-2774555.6	16.1
		-4421.48214	-2774524.3	47.5
Pt-PTA	2	-4435.98128	-2783622.6	0.0
	4	-4435.95388	-2783605.4	17.2
	6	-4435.94308	-2783598.6	24.0
		One $^{d}O_2$		
Mn-PTA	5	-4420.84582	-2774125.0	0.0
Fe-PTA	6	-4440.34505	-2786360.9	0.0
Co-PTA	3	-4461.91724	-2799897.7	16.3
	5	-4461.94322	-2799914.0	0.0
Ni-PTA	4	-4486.11764	-2815083.7	0.0
Re-PTA	1	-4396.18272	-2758648.6	0.0
	3	-4396.10170	-2758597.8	50.8
	5	-4396.00798	-2758539.0	109.7
Ru-PTA	2	-4410.80411	-2767823.7	0.0
	4	-4410.79059	-2767815.2	8.5
	6	-4410.74281	-2767785.2	38.5
Rh-PTA	1	-4426.32702	-2777564.5	15.3
	3	-4426.32197	-2777561.3	18.5
	5	-4426.35144	-2777579.8	0.0
Pd-PTA	2	-4443.49566	-2788338.0	5.0
	4	-4443.50367	-2788343.0	0.0
	6	-4443.49881	-2788339.9	3.1
Os-PTA	2	-4408.03006	-2766082.9	0.0
	4	-4407.98884	-2766057.1	25.9
	6	-4407.90816	-2766006.5	50.6
Ir-PTA	1	-4421.57492	-2774582.5	1.1
	3	-4421.57664	-2774583.6	0.0
	5	-4421.56093	-2774573.7	9.9
Pt-PTA	2	-4435.92422	-2783586.8	0.0
	4	-4435.91863	-2783583.3	3.5
		One CO		
Mn-PTA	1	-4497.12432	-2821990.5	38.1
	3	-4497.16143	-2822013.8	14.8
	5	-4497.18505	-2822028.6	0.0
Fe-PTA	2	-4516.66332	-2834251.4	8.7
	4	-4516.66232	-2834250.8	9.3

	6	-4516.67715	-2834260.1	0.0
Co-PTA	1	-4538.29646	-2847826.4	0.0
	3	-4538.27418	-2847812.4	14.0
	5	-4538.27340	-2847811.9	14.5
Ni-PTA	2	-4487.08572	-2815691.2	0.0
	4	-4487.05084	-2815669.3	21.9
Re-PTA	1	-4359.01450	-2735325.2	0.0
	3	-4359.00950	-2735322.1	3.1
	5	-4359.00051	-2735316.4	8.8
Ru-PTA	2	-4487.08572	-2815691.2	0.0
	4	-4487.05084	-2815669.3	21.9
	6	-4487.05085	-2815669.3	21.9
Rh-PTA	1	-4502.71315	-2825497.5	0.0
	3	-4502.68020	-2825476.9	20.7
	5	-4502.62836	-2825444.3	53.2
Pd-PTA	2	-4406.62236	-2765199.6	0.0
	4	-4406.60084	-2765186.1	13.5
Os-PTA	2	-4484.27338	-2813926.4	0.0
	4	-4484.20954	-2813886.3	40.1
	6	-4484.12981	-2813836.3	90.1
Ir-PTA	1	-4497.91688	-2822487.8	0.0
	3	-4497.86748	-2822456.8	31.0
	5	-4497.78807	-2822407.0	80.8
Pt-PTA	2	-4512.30149	-2831514.3	0.0
	4	-4512.24197	-2831477.0	37.4
		One CO_2		
Mn-PTA	1	-4459.12126	-2798143.2	55.1
	3	-4459.16282	-2798169.3	29.1
	5	-4459.20911	-2798198.3	0.0
Fe-PTA	2	-4478.66166	-2810405.0	21.4
	4	-4478.68472	-2810419.5	7.0
	6	-4478.69583	-2810426.4	0.0
Co-PTA	1	-4500.28927	-2823976.5	6.7
	3	-4500.29996	-2823983.2	0.0
	5	-4500.28796	-2823975.7	7.5
Ni-PTA	2	-4487.08572	-2815691.2	0.0
	4	-4487.05084	-2815669.3	21.9
Ru-PTA	2	-4449.05354	-2791825.6	0.0
	4	-4449.04539	-2791820.5	5.1
	6	-4449.02519	-2791807.8	17.8
Rh-PTA	1	-4464.67014	-2801625.2	0.0
	3	-4464.66358	-2801621.0	4.1
	5	-4464.63687	-2801604.3	20.9
Rh-PTA	1	-4502.71315	-2825497.5	0.0

	3	-4502.68020	-2825476.9	20.7
	5	-4502.62836	-2825444.3	53.2
Pd-PTA	2	-4481.87511	-2812421.5	0.0
	4	-4481.86364	-2812414.3	7.2
Re-PTA	2	-4484.27338	-2813926.4	0.0
	4	-4484.20954	-2813886.3	40.1
Os-PTA	2	-4446.17477	-2790019.1	0.0
	4	-4446.16263	-2790011.5	7.6
	6	-4446.12821	-2789989.9	29.2
Ir-PTA	1	-4459.81844	-2798580.7	0.0
	3	-4459.81168	-2798576.4	4.2
	5	-4459.76560	-2798547.5	33.2
Pt-PTA	2	-4474.24838	-2807635.6	0.0
	4	-4474.22417	-2807620.4	15.2
		One H_2O		
Mn-PTA	1	-4346.97828	-2727772.3	52.5
	3	-4347.02161	-2727799.5	25.3
	5	-4347.06190	-2727824.8	0.0
Fe-PTA	2	-4366.52017	-2740035.1	21.4
	4	-4366.54050	-2740047.8	8.6
	6	-4366.55419	-2740056.4	0.0
Co-PTA	1	-4388.15104	-2753608.7	3.0
	3	-4388.15576	-2753611.6	0.0
	5	-4388.14757	-2753606.5	5.2
Ni-PTA	2	-4412.36651	-2768804.1	0.0
	4	-4412.35015	-2768793.8	10.3
Ru-PTA	2	-4336.91063	-2721454.8	0.0
	4	-4336.90319	-2721450.1	4.7
	6	-4336.88142	-2721436.5	18.3
Rh-PTA	1	-4352.52920	-2731255.6	0.0
	3	-4352.50648	-2731241.3	14.3
	5	-4352.49043	-2731231.3	24.3
Rh-PTA	1	-4369.73309	-2742051.2	0.0
	3	-4369.71663	-2742040.9	10.3
	5	-4322.10867	-2712166.4	0.0
Pd-PTA	2	-4322.10707	-2712165.4	1.0
	4	-4322.09281	-2712156.5	10.0
Re-PTA	2	-4334.03240	-2719648.7	0.0
	4	-4334.02476	-2719643.9	4.8
Os-PTA	2	-4333.98865	-2719621.2	27.5
	4	-4347.67891	-2728212.0	0.0
	6	-4347.67111	-2728207.1	4.9
Ir-PTA	1	-4347.67889	-2728212.0	0.0
	3	-4362.10926	-2737267.2	0.0

	5	-4362.07955	-2737248.5	18.6
Pt-PTA	2	-4346.97828	-2727772.3	52.5
	4	-4347.02161	-2727799.5	25.3

Table S2. The $\boldsymbol{E}_a$ values (in kcal/mol) of RDS for CO and H_2 oxidation in the gas phase, as well as in water, and MeOH at various temperatures (from 250 to 450 K).

Temp. (K)	CO oxidation			H_2 oxidation		
	$\boldsymbol{E}_a$ (gas)	$\boldsymbol{E}_a$ (water)	$\boldsymbol{E}_a$ (MeOH)	$\boldsymbol{E}_a$ (gas)	$\boldsymbol{E}_a$ (water)	$\boldsymbol{E}_a$ (MeOH)
250	33.7	18.5	19.5	38.4	26.1	28.2
275	33.7	18.5	19.5	39.0	26.8	28.8
300	33.7	18.5	19.5	39.7	27.5	29.5
325	33.7	18.5	19.5	40.4	28.2	30.3
350	33.7	18.5	19.5	41.1	28.9	31.0
375	33.7	18.5	19.5	41.8	29.6	31.7
400	33.7	18.4	19.4	42.5	30.3	32.4
425	33.6	18.4	19.4	43.2	31.0	33.2
450	33.6	18.4	19.4	43.9	31.7	33.9

Table S3. The reaction rates (k) of RDS for CO and H_2 oxidation in water and MeOH at various temperatures (from 250 to 450 K).

Temp. (K)	CO oxidation		H_2 oxidation	
	k (water)	k (MeOH)	k (water)	k (MeOH)
250	3.244E-04	4.330E-05	7.340E-11	1.284E-12
275	1.121E-02	1.797E-03	2.831E-09	6.898E-11
300	2.126E-01	3.970E-02	5.789E-08	1.890E-09
325	2.542E+00	5.400E-01	7.489E-07	3.085E-08
350	2.143E+01	5.160E+00	6.758E-06	3.396E-07
375	1.367E+02	3.570E+01	4.448E-05	2.657E-06
400	6.942E+02	1.972E+02	2.353E-04	1.614E-05
425	2.889E+03	8.836E+02	1.003E-03	7.956E-05
450	1.029E+04	3.363E+03	3.690E-03	3.296E-04

Table S4. The Os center's Hirshfeld charges (q, e) and Hirshfeld spin populations (ρ, e) of Os_1/PTA in gas and various solvents.

Gas/ Solvents	Gas	THF	Water	CCl_4	PhH	PhCl	PhMe	ACE	MeOH	MeCN	DMSO	$CHCl_3$
q	0.490	0.743	1.023	0.574	0.576	0.702	0.581	0.898	0.940	0.956	0.920	0.717
ρ	0.870	1.006	1.353	0.885	0.918	0.963	0.887	1.194	1.230	1.255	1.221	0.961